Design of a high precision falling ball viscometer

Matthieu Brizard, Mohamed Megharfi, Claude Verdier, Eric Mahé

DESIGN OF A HIGH PRECISION FALLING BALL VISCOSIMETER

M. Brizard* ; M. Megharfi*; C. Verdier**; E. Mahé*
*Laboratoire National d'Essais (BNM-LNE), 1 rue Gaston Boissier 75015 Paris cedex 15
**Laboratoire de Spectrométrie Physique (UMR5588, UJF-CNRS), 140 avenue de la physique BP 57 38402 S^{t} Martin d'Hères Cedex

Abstract

The increase in uncertainty throughout the viscosity scale being the principal disadvantage of capillary viscometry, the BNM-LNE decided to develop an absolute falling-ball viscometer making it possible to cover a wide range of viscosity while keeping a weak uncertainty. The measurement of viscosity then rests on the speed limit measurement of falling ball, corrected principal identified effects (edge effects, inertial effects, etc). An experimental bench was developed in order to reach a relative uncertainty of the order of 10^{-3} to the measure of viscosity. This bench must allow to observe the trajectory of the ball inside a cylindrical tube filled with liquid for which the viscosity is to be measured, and to obtain the variations in speed throughout the fall in order to determine the area where the speed limit is reached.

Introduction

The measurement of the fluids' viscosity is nowadays important in many industrial processes such as forming of polymers, manufacturing of varnishes, cosmetics, certain food products and various suspensions. There are various measurement techniques like the capillary or rotary rheometry.

The viscosity laboratory of BNM-LNE provides reference oils, and calibrates capillary tube viscometers of all types to ensure the traceability of national standards. Materialization of the national range of viscosity is based on the kinematics viscosity of bi-distilled water at 20°C (1.0034mm².s^{-1}). This value can be used to calibrate primary U-tube viscometers, which are used to calibrate the Ubbelhode type work viscometers.

The main disadvantage of capillary viscosimetry is the increase in uncertainty at each stage of the procedure [1]. This comparative method known as "step up" is based on the water's viscosity which itself is a value measured and subjected to uncertainties [2] but also disputed by a part of the scientific community.

Thus, it is important to install an absolute viscometer, allowing on the one hand to cover a wide range of viscosity measurement while keeping a weak uncertainty, and on the other hand to ensure the traceability to base quantity of the International System.

We decided to develop a method based on the falling ball in a fluid because it is simple to implement and the only one which makes it possible to obtain desired uncertainty. Its operating principle is simple. A rigid solid sphere, with diameter d and density ρ_b, falls under the effect of gravity in the Newtonian liquid study, density ρ and viscosity coefficient η. For Newtonian fluids, the principle of measurement is based on relative balance between the forces of pressure, viscosity and gravity.

The Stokes theory constitutes the theoretical base for the problem. It is valid with very small Reynolds numbers, in steady state and infinite medium.

The falling speed of the ball is then inversely proportional to viscosity, and is given by the expression:

$$\eta = \frac{d^2}{18U_\infty}(\rho_b - \rho)g \qquad (1)$$

with :
η : Fluid dynamic viscosity (Pa.s)
d : Ball diameter (m)
U_∞ : Ball speed limit ($m.s^{-1}$)
ρ_b : Ball density ($kg.m^{-3}$)
ρ : Fluid density ($kg.m^{-3}$)
g : Gravity acceleration ($m.s^{-2}$)

Nevertheless, this equation is valid only when the speed limit is reached, and for a falling sphere in an infinite medium without inertial effects [3]. It is why a certain number of corrections must be applied to the speed U_∞. We can therefore distinguish the corrections due to the inertial effects, the edge effects, the end effects and finally to the rotation of the ball.
This article describes the first development stages of this viscometer. The bibliographical study highlights the various corrections, which must be applied so that the formula connecting viscosity to the falling ball speed in a tube and the associated calculation of uncertainties are valid (§ 1). The following part presents the experimental set-up (§ 2), and finally, the results are presented in the last part (§ 3).

1. Bibliographical Study

The Stokes theory, which allows to express viscosity according to the speed limit of the falling ball applies only if the ball falls in an infinite medium, and to the borderline case where $Re \to 0$ (creeping flows). It is thus necessary to consider the influence of the diameter of the tube as well as that of the Reynolds number. Indeed, the walls and the extremities of the cylinder tend to slow the ball down while the inertial effects increase the falling speed. Moreover, one rough ball can even revolve around itself and shift from the cylinder axis.

1.1. Inertia

A Reynolds number is defined based on the diameter of the ball:

$$Re = \frac{\rho U_\infty d}{\eta}$$

When the inertial effects are negligible, the drag coefficient is written :

$$C_D = \frac{24}{Re} \text{ for } Re \ll 1 \quad (2)$$

Oseen [5] extended the Stokes law by considering the fluid inertia :

$$C_D = \frac{24}{Re}\left(1 + \frac{3}{16}Re\right) \quad (3)$$

This equation gives the value of the drag coefficient for $0 < Re < 1$. This formula was improved by Proudman and Pearson [6], then by Ockendon and Ewans [7] who respectively obtained terms of higher degrees :

$$C_D = \frac{24}{Re}\left(1 + \frac{3}{16}Re + \frac{9}{160}Re^2 \ln\frac{Re}{2} + \frac{0{,}1879}{4}Re^2 + \ldots\right) \quad (4)$$

Goldstein [8] carried out a theoretical analysis on the corrections of inertia in the absence of walls. The following coefficient was obtained :

$$C_D = \frac{24}{Re}\left[1 + a_1 Re - a_2 Re^2 + a_3 Re^3 - a_4 Re^4 + a_5 Re^5 - \ldots\right] \quad (5)$$

with:

$$a_1 = \frac{3}{16} \qquad a_2 = \frac{19}{1280} \qquad a_3 = \frac{71}{20480} \qquad a_4 = \frac{30179}{3440640} \qquad a_5 = \frac{122519}{560742400}$$

These works were verified by those of Shanks [9], who obtained for the 5th term level :

$$a_5 = \frac{122519}{550502400}$$

Maxworthy [10] carried out an experimental study of the inertial effects for $0 < Re < 11$.
Other solutions are available in the literature, abstracted by Clift [3] or Khan and Richardson [11].

1.2. Edge effects

The analytical solution for a sphere of diameter d in translation with a constant speed U_{Stokes} was developed by Stokes [12] within the limit of Re<<1 and in an infinite medium.
In a finite field of diameter D (cylindrical tube of diameter D filled with oil), the effects caused by the rigid walls involve an increase in the viscous dissipation which decreases the sphere's speed [13].
The correction factor due to the wall-attachment effects K(d/D) for a creeping flow of a Newtonian fluid describes the decrease in the speed resulting from the presence of the walls as a function from the ratio of the rays between those of the sphere and the tube (d/D). It is defined in experiments by :

$$K_p(d/D) = \frac{U_{Stokes}}{U_\infty(d/D)} \tag{6}$$

The drag force can thus be defined by :

$$F = 3\pi\eta d U_\infty K$$

Faxen [14] solved the equation of motion while taking into account the boundary conditions simulating the walls and by using the approximation of Oseen [5]. He obtained a coefficient of correction applied to the Stokes force for a sphere falling into a cylinder:

$$K_{pRe} = \frac{F}{F_\infty} = \left[1 - \frac{3}{16}Re - \frac{d}{D}f\left(\frac{Re/4}{d/D}\right) + 2.09\left(\frac{d}{D}\right)^3 - 0.95\left(\frac{d}{D}\right)^5\right]^{-1} \tag{7}$$

where the function f has the following values :
f(0)=2.104 f(0.5)=1.76 f(1)=1.48 f(2)=1.04 f(5)=0.46
Bohlin [15], in a theoretical study using an extension of Faxen's method of reflections obtains the following correction, for Re<<1 and d/D<0.6 :

$$K_p = \left[\begin{array}{l} 1 - 2.10443\left(\frac{d}{D}\right) + 2.08877\left(\frac{d}{D}\right)^3 - 0.94813\left(\frac{d}{D}\right)^5 - 1.372\left(\frac{d}{D}\right)^6 + 3.87\left(\frac{d}{D}\right)^8 \\ - 4.19\left(\frac{d}{D}\right)^{10} ... \end{array}\right]^{-1} \tag{8}$$

In an experimental study, Francis [16] gives for d/D<0.97 and Re<1 :

$$K_p = \left[\frac{1 - 0.475\frac{d}{D}}{1 - \frac{d}{D}}\right]^4 \tag{9}$$

Haberman and Sayre [17] also determined in experiments the coefficient K for d/D<0.8 and Re<2 :

$$K_p = \frac{1 - 0.75857\left(\frac{d}{D}\right)^5}{1 - 2.1050\left(\frac{d}{D}\right) + 2.0865\left(\frac{d}{D}\right)^3 - 1.7068\left(\frac{d}{D}\right)^5 + 0.72603\left(\frac{d}{D}\right)^6} \quad (10)$$

Faxen's formula was confirmed in experiments by Kawata [18], who expressed the wall effects, for d/D<0.07 and Re<1, by :

$$K_p = \left[1 - a_w \frac{d}{D}\right]^{-1} \quad (11)$$

The a_w function has the following values :

a_w=2.104 for d=2.0mm
a_w=2.103 for d=2.4mm
a_w=2.099 for d=3.2mm

Sutterby [19] also carried out experimental works on the wall and inertial effects for 0<d/D<0.13 and 0.0001<Re<3.78.

As a result, an empirical correlation for the wall to wall correction factor :

$$K_p = f(Re, d/D)$$

1.3. Lift force

Dealing with this problem relating to the hypothesis of the creeping flows does not reveal the presence of lift forces tending to move the sphere perpendicularly to the tube axis (Case of a rough sphere revolving around itself).

Calculations of Rubinov and Keller [20] indicate that a sphere in rotation falling into a stationary fluid experiences a lift force F_L which is orthogonal to the motion direction. This force is given by :

$$\vec{F}_L = \pi \frac{d^3}{8} \rho \vec{\Omega} \times \vec{U}\left[1 + O(Re)\right] \quad (12)$$

$\vec{\Omega}$: angular speed of the sphere

$\vec{U}$: sphere speed

For low values of Reynolds numbers, the transverse force is independent from viscosity [20].

Rubinov and Keller [20] tried to apply their results to the problem of the lateral motion of a sphere freely suspended in a Poiseuille flow. The transverse force is always directed in order to bring back the sphere towards the centre of the tube and would be cancelled on the tube axis.

1.4. End effects

The end effects were theoretically studied by Lorentz [21] in a length L tube, without considering the wall effect modelled later by Faxen [14]. For a sphere approaching a rigid infinite plan, he obtained the following correction :

$$K_b = 1 + \frac{9}{8}\frac{d}{2z} \quad (13)$$

where z is the distance between the sphere and the cylinder base.

Tanner [22], reusing the method of reflections taking into account the wall effect, modelled the end effect, and studied its influence on the total drag (Re<<1). He gives the increase in the drag due to end effect according to the 2z/D ratio where z is the distance between the ball and the cylinder base and D the tube diameter.

For Sutterby [19], the corrections due to the end effects are useless for :

$L/D > 2$ Re<2 $d/D < 0.125$

Works of Flude and Daborn [4] confirm the results obtained by Sutterby [19]. Indeed, it is not necessary to apply at the same time the corrections due to the end effects and the corrections due to the edge effects, except if the ball is only a few diameters away from the tube base.

Equation 1 being valid only when the speed limit is reached, and if the sphere falls in an infinite medium without inertial effects, one will use, at first approximation, the coefficient of correction of Faxen (Equation 7) which makes it possible to consider at the same time edge effects and inertial effects. By considering that measurements are taken sufficiently far from the tube extremity, no coefficient relating to the end effects will be applied. Moreover, a possible rotation of the ball will not be taken into consideration.

The expression of viscosity then becomes :

$$\eta = \frac{d^2}{18U_\infty}(\rho_b - \rho)g\left[1 - \frac{3}{16}Re - \frac{d}{D}f\left(\frac{Re/4}{d/D}\right) + 2.09\left(\frac{d}{D}\right)^3 - 0.95\left(\frac{d}{D}\right)^5\right] \quad (14)$$

1.5. Uncertainties calculations on the measurement system

The interest of this study being primarily metrological, it is important to determine uncertainty on the speed measurement system in order to reach the following viscosity measure objective : 10^{-3}.

The expression of the viscosity variance $u^2(\eta)$, by taking into account the previous non correlated parameters becomes :

$$u^2(\eta) = \left(\frac{\partial\eta}{\partial d}\right)^2 u^2(d) + \left(\frac{\partial\eta}{\partial D}\right)^2 u^2(D) + \left(\frac{\partial\eta}{\partial\rho}\right)^2 u^2(\rho) + \left(\frac{\partial\eta}{\partial g}\right)^2 u^2(g) + \left(\frac{\partial\eta}{\partial\rho_b}\right)^2 u^2(\rho_b) + \left(\frac{\partial\eta}{\partial U_\infty}\right)^2 u^2(U_\infty) \quad (15)$$

We then calculate the uncertainty, with which the measurement principle must comply. This calculation is carried out using the parameters of Table 1

Parameter	Value	Standard-Uncertainty	Preponderance (%)
Fluid density ($kg.m^{-3}$)	898	$2.25.10^{-2}$	0
Ball density ($kg.m^{-3}$)	6000	$4.5.10^{-2}$	1.9
Ball diameter (m)	2.10^{-3}	1.10^{-6}	47.7
Tube diameter (m)	10.10^{-2}	1.10^{-6}	0
Falling speed ($m.s^{-1}$)	$9.5.10^{-3}$	$9.5.10^{-6}$	49.9
Gravity acceleration ($m.s^{-2}$)	9.81	91.10^{-8}	0,5
Viscosity (Pa.s) (20 °C)	1.133	$1.416.10^{-3}$	/

Table 1 : Values used for the uncertainty calculation

$$Re = \frac{\rho U_\infty d}{\eta} = 0.01 \qquad f\left(\frac{Re/4}{d/D}\right) = 2.095$$

It is noted that the two dominating parameters when calculating uncertainties are the ball diameter and its falling speed. According to these parameters, the relative uncertainty of the speed measurement system must be of 10^{-3} to obtain a relative uncertainty of 10^{-3} to the viscosity measure. This value thus will enable us to determine the most suitable measurement principle. With regard to the ball diameter, our means of calibration enable us to have an uncertainty-type of 1 µm.

2. Speed measurement method

2.1. Measurement of U_∞

The authors having worked on the falling balls developed various speeds measurement systems. To compare the measurements of viscosity obtained by capillary viscosimetry and with a falling ball viscosimeter, Flude and Daborn [4] used a laser technique with Doppler effect. The sphere speed is continuously measured as it falls into a cylinder filled with oil. Arigo and McKinley [23] visualized the falling ball using a fixed camera. Lommatzsch [24] proposed the following measurement method : the camera is given a speed close to that of the ball.

The ball speed ($\vec{U}_\infty$) is then determined by the sum of its speed in the field of the camera ($\vec{U}_{bc}$) and the camera speed ($\vec{U}_c$) :

$$\vec{U}_\infty = \vec{U}_{bc} + \vec{U}_c \qquad (16)$$

As for Tran-Son-Tay [25] and Mordant and Pinton [26] they developed systems of acoustic measurement based on the Doppler effect of an ultrasonic wave returned by the falling particle. In comparison with the various methods already used, it was thus decided to develop a method using a line scan CCD camera. The linear camera makes it possible to obtain very high resolutions and frequencies of acquisition and give us the possibility of taking quasi-instantaneous speed measurements. This technique enables us to measure the variations in the ball speed along the tube and to observe its trajectory.

Finally, the stages allow us to move along the tube (Figure 1).

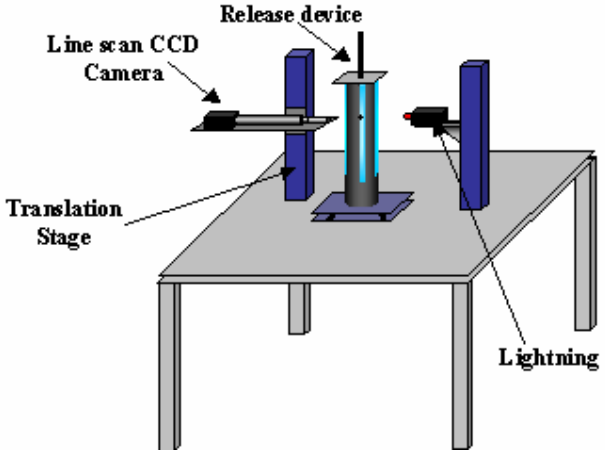

Figure 1 : Diagram of the experimental set-up

2.2. Experimental set-up

This part presents the various options chosen concerning the assembly of the experimental set-up. The video system of measurement must enable us to observe a ball of 2 mm out of 2000 pixels with a resolution of 1 pixel.

The camera used comes from the Lord Ingenierie Company (Corbreuse) associated with a video acquisition board National Instruments (PXI 1422) (Le Blanc-Mesnil). It is made of a 5150 pixel linear CCD sensor and a line frequency going up to 3.7 Khz.

In order to exploit the camera's possibilities, Silloptics Company provided the used lens (Wendelstein, Germany). This telecentric lens fitted with an extension tube, which has an enlargement x10. Monochromatic and shadowscopic lighting makes it possible to observe the ball with well-contrasted edges. For this purpose, a red LED provided with a condenser moves facing the camera.

The aluminium tube was treated in order to make it matt and to reduce the parasitic reflections of light. Four openings were cut out facing the cameras and lightings in order to place plane plates of glass making it possible to reduce the optical deformations which would have generated a tube out of traditional cylindrical glass.

The camera must move along the tube in order to follow the ball. To do so we use a Micro-control (IMS300) (Evry) stage provided with a direct current engine. This stage makes it possible to move the camera at a distance of 300 mm, but generates errors of positioning due to the pitch, roll and yaw angles [27-28].
Indeed the stage has a ball bearing guidance system and a precision ballscrew drive. However, a ball guidance is not repeated on the scale of the micrometer. It is consequently important to be able to correct the stage's defects.
The measurement of the hunting will be made with the assistance of an electronic level, which directly gives us the value of the angle. The measurement of the roll angle is made with the assistance of two length gauges. These length gauges are placed facing a reference surface (Granite block). One calculates the camera's angle of rotation by knowing the distance between the detectors and the displacement measured by each one of them. Finally, pitch angle is measured with another electronic level (Figure 2).

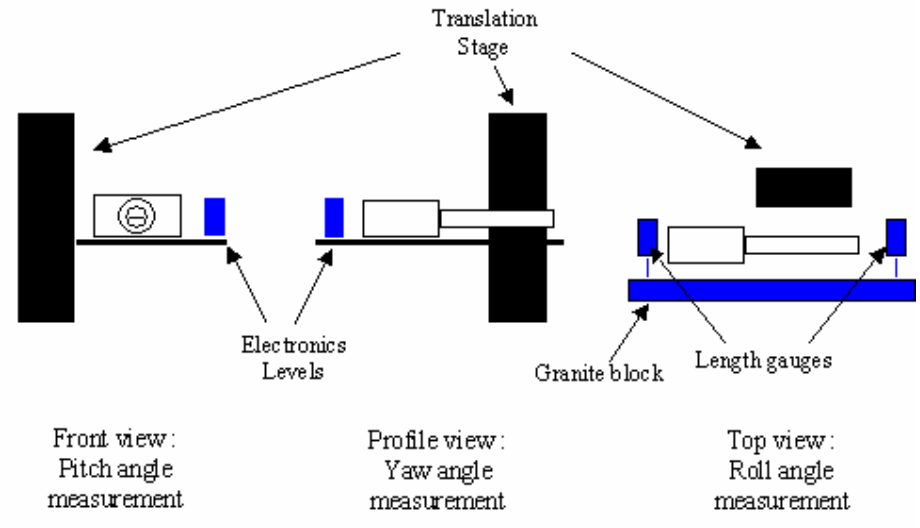

Figure 2 : Pitch, roll and yaw angles measurement

The balls used must be selected so as to keep very low Reynolds numbers. The tests will be carried out with ceramics balls, glass balls…
In order to maintain the ball in oil and to release it at rest in the centre of the tube, we developed an aspiration release device. This method thus enables us to use any ball materials to carry out the tests, contrary to an electromagnet. A device then enables us to accurately position the ball in the centre of the tube. Finally, the temperature is controlled with the assistance of a 25 Ohms platinum probe. Finally, all the instruments are interfaced under LabView. Figure 3 shows the bench described previously.

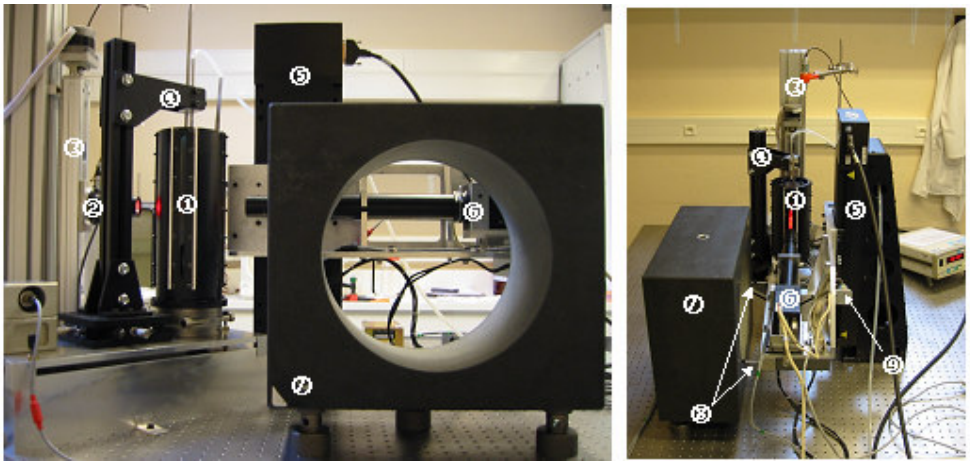

Figure 3 : Experimental bench

①: Cylindrical tube
②: Lighting
③: Stage allowing lighting displacement
④: Ball releasing device
⑤: Stage allowing camera control
⑥: Camera
⑦: Granite Block
⑧: Detectors
⑨: Electronic Levels

3. Experimental results

3.1. The system used

First measurements were taken for two batches of oil and for different temperatures. Table 2 presents the values of the various parameters and their associated uncertainties.

	Value	Uncertainty
d (m)	$2.000.10^{-3}$	1.10^{-6}
D (m)	$9.947.10^{-2}$	1.10^{-6}
ρ_b (kg.m^{-3})	3963	2
g (m.s^{-2})	9.81	91.10^{-8}
P (kg.m^{-3}) 350 (1st batch) 22.389 °C	895	2
ρ (kg.m^{-3}) 350 (2nd batch) 19.149 °C	887	2
P (kg.m^{-3}) 350 (2nd batch) 21.114°C	885	2
ρ (kg.m^{-3}) 350 (2nd batch) 24.617 °C	884	2

Table 2 : Parameters

3.2. Speed measurement

The following image (Figure 4) presents the ball seen by the line scan camera when passing in front of the lens at the time of its fall. The position of the ball edge is given by finding the point where the gradient of grey level is maximum. This data enables us to measure the ball diameter and to obtain the barycentre position. By knowing the time interval between two images and the displacement of the barycentre, the falling ball speed is obtained.

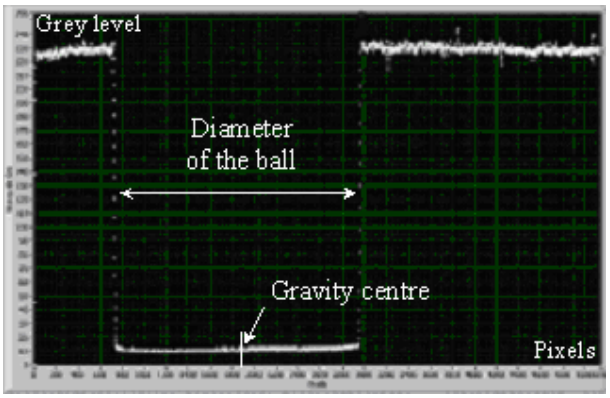

Figure 4 : Ball passage

Several measurements are taken along the tube. The camera remains fixed and in order to measure the ball speed in the field of the camera. Once the ball has passed, the camera is displaced for the following measurement.
Seven measurements are made along the tube. The first one is made just after its release and the following ones are every 3 cm.
The first measurement makes it possible to feature the transient of the ball, the others give the speed limits reached by the ball (Figure 5).

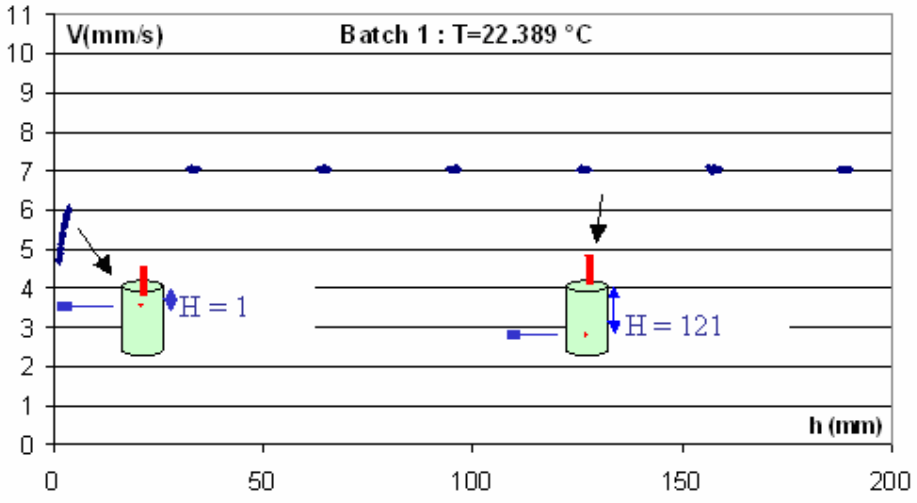

Figure 5 : Variations in the ball's speed (acquisitions at 100 Hz)

3.3. Results

Table 3 summarises the measurements made all along the fall for various frequencies of acquisitions, when the ball reaches its speed limit. The speed value is calculated from the average of the results obtained for each measurement.

	1000 Hz		100 Hz		10 Hz	
	Speed (mm/s)	**Standard deviation**	**Speed (mm/s)**	**Standard deviation**	**Speed (mm/s)**	**Standard deviation**
Measurement 1	7.03	0.11	7.05	0.08	7.050	0.002
Measurement 2	7.06	0.1	7.06	0.01	7.051	0.003
Measurement 3	7.05	0.09	7.05	0.02	7.048	0.001
Measurement 4	7.04	0.08	7.04	0.02	7.047	0.004
Measurement 5	7.04	0.09	7.04	0.03	7.040	0.002

Measurement 6	7.03	0.1	7.04	0.01	7.043	0.003

Table 3 : Measurement results

$U_\infty = 7.045 \pm 0.012$ mm.s^{-1} (k=1)

Therefore, the obtained viscosity is :

$$\boxed{\eta = 0.909 \pm 0.002 \text{ Pa.s}} \text{ (k=1)}$$

By using a capillary viscosimeter, the obtained viscosity, for the same temperature is :

$$\boxed{\eta = 0.908 \pm 0.004 \text{ Pa.s}} \text{ (k=1)}$$

3.4. Viscosity measurements at other temperatures

Complementary tests were conducted at 19.149°C, 21.114°C and 24.617°C by using a second oil and a 2-mm diameter ceramic ball. The results obtained are shown in figure 6 and are compared with the value of viscosity obtained by measurement with a capillary tube viscometer (Table 4).

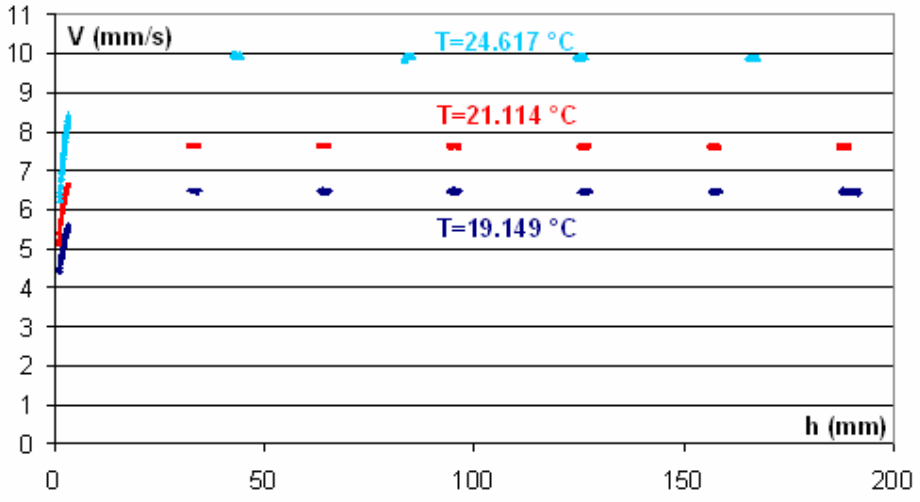

Figure 6 : Falling speed of a 2 mm- ceramics ball in a 350-oil (Batch 2) at 19.149°C, 21.114°C and 24.617°C

	Falling ball viscosimeter		**Capillary viscosimeter**	
Temperature °C	*Viscosity (Pa.s)*	*Standard-Uncertainty (Pa.s) (k=1)*	*Viscosity (Pa.s)*	*Standard-Uncertainty (Pa.s) (k=1)*
19.149	0.987	0.002	0.985	0.004
21.114	0.843	0.002	0.842	0.004
24.617	0.644	0.002	0.644	0.004

Tableau 4 : Comparison between the results obtained by capillary viscometer and the falling-ball viscometer.

.

These first results make it possible to obtain the variations in the falling speed of the ball along the tube, with high frequencies (1000 Hz and 100 Hz), the possibility of taking transitional measurements and consequently following the speed variations, and for weaker frequencies (10 Hz), the possibility of having excellent uncertainties on the speed measurement (standard deviation of repeatability ranging between 0.001 and 0.004 mm.s^{-1}).

The results are in perfect compliance with those obtained by capillary viscometry. If the values obtained are compared, a 0.2 % variation is obtained.

Conclusions

The experimental bench of viscosity measurement was designed so as to follow the trajectory of the ball, to obtain the speed evolution throughout the fall, to achieve the goals in terms of uncertainties and to make it possible to ensure the basic sizes traceability of measurements of the International System base quantity. The results obtained show that the principle of measurement perfectly complies with our expectations. In fact, at the time of the same experiment, we could highlight the acceleration of the ball as well as the area where its speed limit of the fall is reached. The use of a linear camera enables us to take measurements at high frequency while keeping an excellent resolution. Finally, this method of absolute measurement enables us to reduce the uncertainties obtained by capillary viscometry.

Acknowledgments : This work was carried out within the framework of a CIFRE thesis in partnership with the Laboratoire de Rhéologie in Grenoble and the support from the BNM. The authors would like to thank their colleagues from the workgroup for their useful comments during the course of this work : Mrs C. Graciannette, Mr D. Jouin, Mr P. Lacipierre, Mr R. Morice and Mrs F. Ollier.

Bibliography

[1] Megharfi M., Devin E. and Moro J.F. La matérialisation de l'échelle de viscosité au BNM-LNE. Bulletin du bureau national de la métrologie. 47-59 (1996).

[2] Collings A.F. and Bajenov V. A high precision capillary viscometer and further relative results for the viscosity of water. Metrologia. 66, 61-66 (1983).

[3] Clift R., Grace J.R. and Weber M.E. Bubbles, drops and particles. Academic Press. New York / London (1978).

[4] Flude and Daborn. Viscosity measurement by means of falling spheres compared with capillary viscometry. J. Phys. E : Sci. Instrum. 15, 1313-1321 (1982).

[5] Oseen C.W. Neuere Methoden und Ergebnisse in der Hydrodynamik. Akademische Verlagsgesellschaft. Leipzig. 10 (1927).

[6] Proudman I. and Pearson J.R.A. Expansion at small Reynolds numbers for the flow past a sphere and a circular cylinder. J-Fluid.Mech. 2, 237-262 (1957).

[7] Ockendon J.R. and Ewans G.A. The drag on a sphere in low Reynolds number flow. Aero. Sci. 3, 327 (1972).

[8] Goldstein S. The steady flow of viscous fluid past a fixed spherical obstacle at small Reynolds numbers. Proc. R. Soc. London A. 123 A, 225-235 (1929).

[9] Shanks D. Non-linear transformations of divergent and slowly convergent sequences. J. Math. Physics. 34, 1-42 (1995).

[10] Maxworthy T. Accurate measurements of sphere drag at low Reynolds numbers. J. Fluid. Mech. 23, 369-372 (1965).

[11] Khan A.R. and Richardson J.F. The resistance to motion of a solid sphere in a fluid. Chem. Eng. Comm. 62, 135-150 (1987).

[12] Stokes G.C. On the effect of internal friction of fluids on the motion of pendulums. Trans. Cambridge Phil Soc. 9, 8-106 (1851) (Mathematical and Physical Papers 3, 1-141 (1901)).

[13] Arigo M. T. and McKinley G.H. The steady and transient motion of a sphere through a viscoelastic fluid. ASME FED. 194, 139-147 (1994).

[14] Faxen H. Die Bewegund einer starren Kugel längs der Achse eines mit zäher Flüssigkeit gefüllten Rohres. Arkiv för matematik, Astronomi och Fysic. 17, 1-28 (1922).

[15] Bohlin X. On the drag on a rigid sphere moving in a viscous fluid inside a cylindrical tube. Trans Roy. Inst. Teck. 155, 1-63 (1960).

[16] Francis A.W. Wall effect in falling ball method for viscosity. Physics. 4, 403-406 (1933).

[17] Haberman W.L., Sayre R.M., Motion of rigid and fluid spheres in stationary and moving liquids inside cylindrical tubes. David Taylor Model Basin report. 1143 (1958).

[18] Kawata M., Kurase K. and Yoshida K. Realisation of a viscosity standard. Proceeding of the 5th international congress on Rheology. 1, 453-472 (1963).

[19] Sutterby J.L. Falling sphere viscometry. Wall and inertial corrections to Stokes' law in long tubes. Trans. Soc. Rheol. 17, 559-573 (1973).

[20] Rubinow S.I. and keller J.B. The transverse force on a spinning sphere moving in a viscous fluid. J. Fluid. Mech. 11, 447-459 (1961).

[21] Lorentz H.A. Abhand. Theor. Phys. 1, 23 (1907).

[22]Tanner R.I. End effects in falling-ball viscometry. J. Fluid Mech. 17, 161-170 (1963).

[23] Arigo M.T., Shapley N., McKinley G.H., Rajagoplan D. The Sedimentation of a sphere through an elastic fluid. Part1. Steady Motion. J. Non-Newtonian Fluid Mech. 60, 225-257 (1995).

[24] Lommatzsch T., Megharfi M., Mahe E., Devin E. Conceptual study of an absolute falling ball viscometer. Metrologia. 38, 531-534 (2001).

[25] Tran-Son-Tay R., Beaty B.B., Acker D.N., Hochmuth R.M. Magnetically driven, acoustically tracked, translating-ball rheometer for small, opaque samples. Review Sci. Instrum. 59, 1399-1404 (1988).

[26] Mordant N., Pinton J.F. Velocity measurement of a settling sphere. Eur. Phys. J. B. 18, 343-352 (2000).

[27] David J.M., Leleu S., Diolez G., Roux T. Evaluation de la géométrie des machines : Présentation d'une méthode innovante. 10ème Congrès International de Métrologie. (2001).

[28] Slocum A.H. Precision machine design : Macromachine design philosophy and its applicability to the design of micromachines. Micro Electro Mechanical Systems. 92, 37-42 (1992).